

An Improved GaAs FET Nonlinear Model Suitable for Intermodulation Analysis of Amplifiers, Switches and Resistive Mixers

J.R. Loo-Yau, J. E. Zúñiga-Juárez, F. I. Hirata-Flores and J.A. Reynoso-Hernández

Centro de Investigación Científica y de Educación Superior de Ensenada (CICESE) División de Física Aplicada, Km. 107 Carretera Tijuana-Ensenada, 22860 Ensenada, B.C. México; emails: rloo@cicese.mx, ezuniga@cicese.mx, fhirata@cicese.mx and apolinar@cicese.mx

Abstract -- This paper presents an $I_{DS}(V_{GS}, V_{DS})$ model to represent PHEMT behavior in the reverse ($V_{DS} < 0$), and forward zone ($V_{DS} > 0$). The model predicts with high accuracy the measured data as well as higher orders derivatives of the transconductance over a large range of V_{DS} bias. These characteristics are important for the analysis of intermodulation distortion using harmonic balance or Volterra series. Using the improved $I_{DS}(V_{GS}, V_{DS})$ model along with an empirical model to simulate the nonlinear behavior of gate-source capacitance, C_{GS} , and gate-drain capacitance, C_{GD} , a GaAs FET nonlinear model suitable for intermodulation analysis of amplifiers, switches and resistive mixers is presented

I. INTRODUCTION

Accurate linear and nonlinear models of MESFET, HEMT and PHEMT are needed in the development of monolithic microwave integrated circuits (MMICs), since tunability in this technology is limited. Control circuits such as SPDT (switches), attenuators and low distortion mixers (resistive mixers) are examples of new applications of MMICs. A good GaAs FET nonlinear model must be capable of describing the transistor behavior in the saturation region for amplifiers, linear region for control circuits, and reverse zone for resistive mixer applications.

A common problem encountered in microwave circuit using GaAs FET is the intermodulation distortion (IMD). IMD phenomena are produced by transistor nonlinearities such as $I_{DS}(V_{GS}, V_{DS})$, $C_{GS}(V_{GS}, V_{DS})$ and $C_{GD}(V_{GS}, V_{DS})$. However, $I_{DS}(V_{GS}, V_{DS})$ is considered the more important nonlinearity giving rise to the distortion phenomenon. Many different models have been developed for modeling the $I_{DS}(V_{GS}, V_{DS})$ characteristics of PHEMT's operated in the forward region ($V_{DS} > 0$, $I_{DS} > 0$) [1]-[6]. In applications such as resistive mixers, the transistor is driven by an RF signal from the forward region ($V_{DS} > 0$, $I_{DS} > 0$) to the reverse region ($V_{DS} < 0$, $I_{DS} < 0$). For this kind of application some of the classical models referenced above fail to predict the $I_{DS}(V_{GS}, V_{DS})$ curves in the reverse zone, as well as the higher order derivatives of transconductance and conductance, so that new models are needed.

Based on Chen *et al* [3] model for a GaAs FET, an improved $I_{DS}(V_{GS}, V_{DS})$ nonlinear model suitable for analyzing high gain amplifiers, switches (SPDT), or resistive mixers is presented in this work. The $I_{DS}(V_{GS}, V_{DS})$ model allows accurate prediction of the higher order derivatives of the transconductance, G_m , with respect to the gate-to-source voltage V_{GS} , in the forward and reverse zone. The parameters of the model can be obtained directly from the $I_{DS}(V_{GS}, V_{DS})$ curve measurements, and the extraction procedure is simple. Furthermore, using the empirical model [11] for modeling $C_{GS}(V_{GS}, V_{DS})$ and $C_{GD}(V_{GS}, V_{DS})$ along with the improved $I_{DS}(V_{GS}, V_{DS})$ model, a nonlinear model suitable for intermodulation analysis of amplifiers, switches and resistive mixers is also presented.

II. THE NEW $I_{DS}(V_{GS}, V_{DS})$ MODEL

The model proposed in [3] calculates the I - V curves and its higher order derivatives for $V_{DS} > 0$ as follows:

$$I_{DS}(V_{GS}, V_{DS}) = (I_{max}^{-1} + I_{dso}^{-1})^{-1} \quad (1)$$

$$I_{max}(V_{DS}) = IPK \cdot \tanh\left(\frac{V_{DS}}{VK}\right) \cdot (1 + \lambda V_{DS}) \quad (2)$$

$$I_{dso} = \exp(\psi) \quad (3)$$

$$\psi(V_{GS}, V_{DS}) = \sum_{i=0}^m a_i V_{GS}^i \quad (4)$$

$$a_i(V_{DS}) = \sum_{j=0}^n a_{ij} V_{DS}^j \quad (5)$$

The model is suitable for analyzing amplifiers; however, it fails in the analysis of the resistive mixer, where the transistor works with $V_{DS} \leq 0$. Under this condition, all the coefficients a_{ij} in (5) are complex number. Therefore, a poor prediction of the IMD during

large signal analysis is expected. In other words, the model is inappropriate for analyzing the performance of resistive mixers designed with PHEMT devices. To overcome this problem, it is necessary to understand why the a_{ij} becomes complex. The coefficients a_{ij} in (5) arise from the two polynomials of Eqs. (4-5). This suggests to consider the function ψ . So, combining Eqs. (1) and (3), $\psi(V_{GS}, V_{DS})$ can be calculated as

$$\psi(V_{GS}, V_{DS}) = \ln\left(\frac{I_{DS} I_{max}}{I_{max} - I_{DS}}\right) \quad (6)$$

It should be noted that (6) becomes complex number when the argument of the natural logarithm takes negative values, and this happens when the transistor is biasing at $V_{DS} < 0$, because $I_{DS}(V_{GS}, V_{DS}) < 0$ also becomes negative. To avoid ψ becoming complex number, it is necessary that:

$$\frac{I_{DS} I_{max}}{I_{max} - I_{DS}} > 0 \quad (7)$$

Our experiments show that $-1 \leq \frac{I_{DS} I_{max}}{I_{max} - I_{DS}} \leq 0$, and to satisfy (7), a new function ψ is proposed as

$$\psi(V_{GS}, V_{DS}) = \ln\left(\frac{I_{DS} I_{max}}{I_{max} - I_{DS}} + 1\right) \quad (8)$$

and therefore

$$I_{dso} = \exp(\psi) - 1 \quad (9)$$

With this modification, the model predicts the $I_{DS}(V_{GS}, V_{DS})$ curves from the reverse to the forward region as well as the higher order derivatives of G_M and G_{DS} .

III. RESULTS

On-wafer PHEMTs with gate length of $L_g = 0.25 \mu m$ were used in this study. A LRM (Line-Reflect-Match) calibration was performed on a HP8510C network analyzer using picoprobes (model 50A-GSG-150P). DC measurements were performed at room temperature using a computer controlled measurement system formed with Tektronix equipment (models PS5004, PS5010 and DM5120).

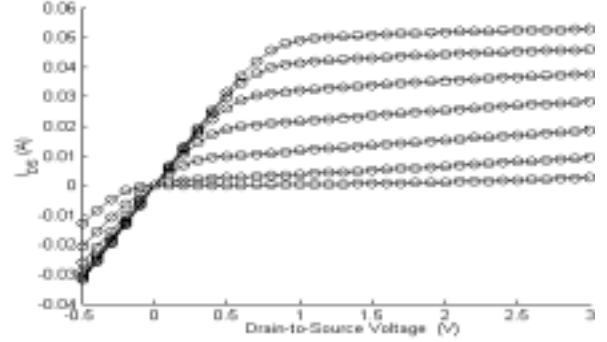


Fig. 1. DC curves for a HP PHEMT. V_{DS} range from: -0.5 to 0.5 linear step of 0.1V, $V_{GS} = -0.8, -0.6, -0.4, -0.2, -0.1, 0, 0.2,$ and 0.4V. Measured (dot), solid (simulated)

To validate the improved model, we compared the measured $I_{DS}(V_{GS}, V_{DS})$ curves and their higher order derivatives with the values predicted by the model. As mentioned in the last section, the model predicts well the $I_{DS}(V_{GS}, V_{DS})$ curves as well as their higher order derivatives. Fig. 1 shows the experimental data along with the modeling of $I_{DS}(V_{GS}, V_{DS})$ for values from V_{DS} of -0.5V to 3V. On the other hand, Figs. 2 show the measured and simulated of transconductance, G_M . To accomplish the DC validation, figures 4(a) - 4(c) show the modeling of the first and second derivatives of the transconductance at three different V_{DS} . Once the I/V model had been validated, the second step was to code the new model in ADS, in order to be used in the nonlinear equivalent circuit model presented in Figs.3. Prior to C_{GS} and C_{GD} extraction, parasitic capacitances C_{PG} and C_{PD} were extracted using the Dambrine procedure [8]. The parasitic resistances R_S, R_D, R_G and the parasitic inductances L_S, L_D and L_G were determined following the Reynoso method [9]. Once all parasitic elements were extracted, the intrinsic elements were determined using the Berroth and Bosh method [10]. To simulate the nonlinear behavior of $C_{GS}(V_{GS}, V_{DS})$ and $C_{GD}(V_{GS}, V_{DS})$ we used the model proposed in [11]. The nonlinear equivalent circuit model shown in figure 3a was used to simulate the reverse and linear region, and the one presented in figure 3b was used to simulate the saturation region. To take into account the dispersion of the output conductance, a parallel $R_{ds} - C$ branch was added [12].

In figure 5(a) - 5(d) we compare the measured S_{ij} at different V_{DS} with the S_{ij} predicted by the PHEMT nonlinear model. Good agreement between the simulated behavior and the experimental data is achieved up to 50 GHz. Finally in figure 6-7 shows the simulated power performance (harmonics) of the PHEMT biased at $V_{DS} = 0.2, 0.4, 1.4$ and 1.6V. The results in figure 7 show an error in the second and the third harmonic, thermal effects related with deep level trap could be an hypothesis to explain this error. All the simulation was performed at $V_{GS} = -0.45V$ and at 5GHz.

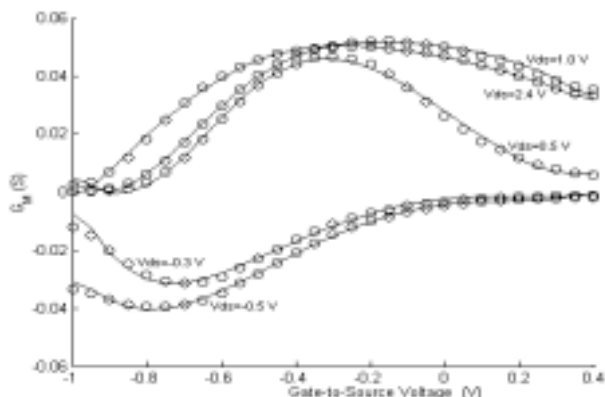


Fig. 2. Measured (dot) and modeled (solid) G_M Vs V_{GS} , $V_{DS} = -0.5, -0.3, 0.5, 1.0, \text{ and } 2.4V$.

IV. CONCLUSIONS

A new nonlinear GaAs FET model for $I_{DS}(V_{GS}, V_{DS})$ has been introduced. The main feature of the model is its ability to predict the PHEMTs I/V characteristics in the reverse zone. Furthermore, the model predicts the $I_{DS}(V_{GS}, V_{DS})$ curves and their derivatives with high accuracy. These characteristics make the model very attractive for application in the design of amplifiers, switches and resistive mixers. Simulation with ADS show good agreement with measured S parameters in the reverse and forward region.

ACKNOWLEDGEMENTS

The authors thank Jesús Ibarra and Benjamin Ramirez for his assistance during the measure the $P_{in} - P_{out}$. This work was supported by a joint funding of CICESE and CONACyT of Mexico.

REFERENCES

- [1] W. Curtice and M. Etteberg, "A Nonlinear GaAs FET Model for Use in the Design of Output Circuits for Power Amplifiers," *IEEE Trans. Microwave Theory Tech.*, vol MTT-33, no 2, pp. 1383, 1985.
- [2] I. Angelov, H. Zirath, and N. Rorsman, "A New Empirical Model for HEMT and MESFET Devices," *IEEE Trans. Microwave Theory Tech.*, vol 40, no 12, pp. 2258-2266, December 1992.
- [3] Y. C. Chen, D. L. Ingram, H. C. Yen, R. Lai, and D. C. Streit, "A New Empirical I-V for HEMT Devices," *IEEE Microwave and Guided Letters*, vol. 8, no 10, pp.342-344, October 1998.
- [4] T. Fernández, J.A. García, A. Mdiavilla, J. C. Pedro, and J. L. García, "Accurately Modeling the Drain to Source Current in Recessed Gate P-HEMT Devices," *IEEE-Electron Device Letters*, vol 20, no 11, pp.557-559, November 1999.

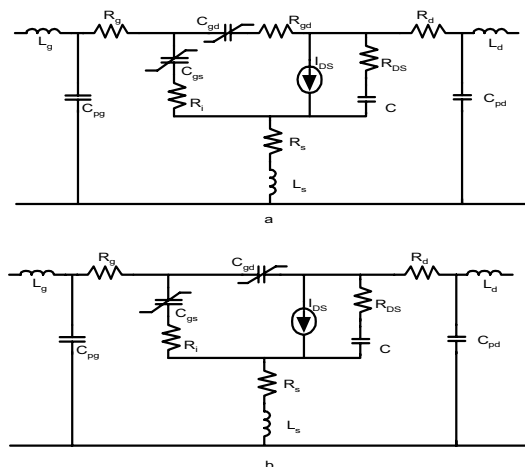


Fig. 3. Nonlinear equivalent circuit: a) $-0.5V < V_{DS} < 0.5$; b) $V_{DS} > 0.5V$

- [5] Klas Yhland, Niklas Rorsman, Mikael Garcia, and Harald F. Merkel, "A Symmetrical Nonlinear HFET/MESFET Model Suitable for Intermodulation Analysis of Amplifiers and Resistive Mixers," *IEEE Trans. Microwave Theory Tech.*, vol MTT-48, no 1, pp.15-22, January 2000.
- [6] Guoli Qu, and Anthony E. Parker, "New Model Extraction for Predicting Distortion in HEMT and MESFET Circuits," *IEEE Microwave and Guided Wave Letters*, vol 9, no 9, pp.363-365, September 1999.
- [7] S. Maas and D. Neilson, "Modeling of MESFET's for Intermodulation Analysis of Mixers and Amplifiers," in 1990 *IEEE-S Microwave Symp. Dig.*, pp. 1291-1294.
- [8] G.Dambrine, A. Cappy, F. Heliodore, E. Playez, "A New Method for Determining the FET Small-Signal Equivalent Circuit," *IEEE Trans. Microwave Theory Tech*, vol 36, pp.1151-1159, July 1988.
- [9] Reynoso H, J. Apolinar, Rangel Patiño, Francisco, and Perdomo, Julio, "Full RF Characterization for Extraction the Small Signal Equivalent Circuit in Microwave FET's," *IEEE Trans. Microwave Theory Tech*, vol 44, pp.2265-2233, December 1996.
- [10] Berroth, M and Bosch, R, "Broad-Band Determination of the FET Small-Signal Equivalent Circuit," *IEEE Trans. Microwave Theory Tech*, vol 38, pp.891-895, July 1990.
- [11] J. R. Loo Yau, R. Infante Galindo, and J. A. Reynoso Hernández, "A New Empirical Gate Capacitance Model for PHEMT and MESFET Transistors," Presented at *58th Automatic Radio Frequency Techniques Group Conf.*, November 2001.
- [12] I. Angelov, "Extraction of the capacitive and dispersive part of the Chalmers model," Chalmers Univ. Technol., Göteborg Sweden, Rep. N26B, 19

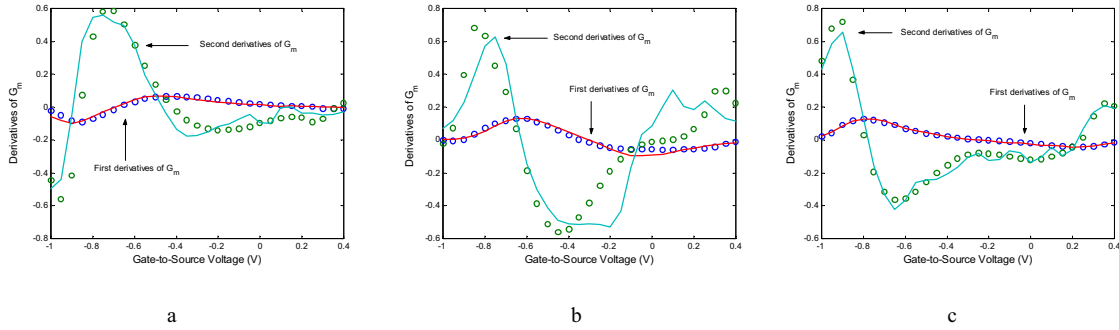


Fig. 4. First and second derivatives of G_M . a) $V_{DS} = -0.3V$, b) $V_{DS} = 0.4V$, c) $V_{DS} = 2.4V$.

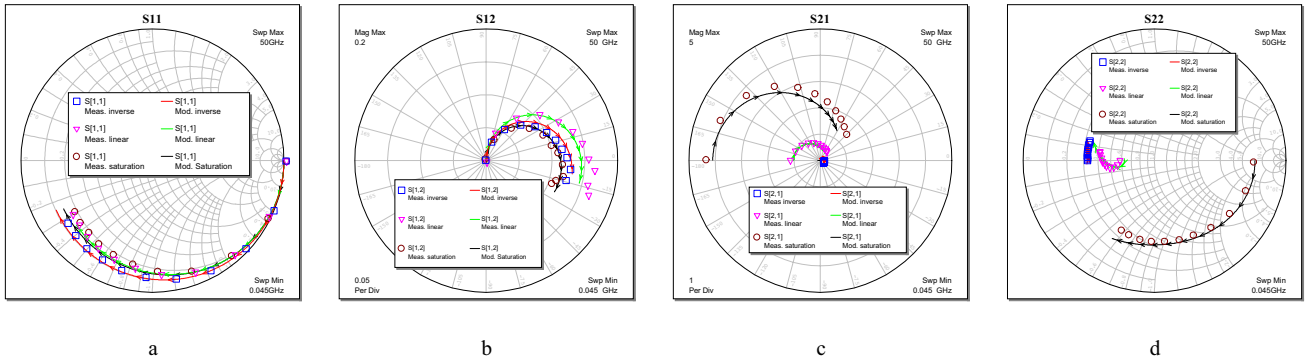


Fig. 5. S parameters results, a) S_{11} @ $V_{DS} = -0.3V$, $V_{GS} = -0.15V$ measured (\square) and modeled (solid); S_{11} @ $V_{DS} = 0.4V$, $V_{GS} = -0.15V$ measured (\square) and modeled (solid), S_{11} @ $V_{DS} = 2.6V$, $V_{GS} = 0V$ measured (\square) and modeled (solid); b) S_{12} @ $V_{DS} = -0.3V$, $V_{GS} = -0.15V$ measured (\square) and modeled (solid); S_{12} @ $V_{DS} = 0.4V$, $V_{GS} = -0.15V$ measured (\square) and modeled (solid), S_{12} @ $V_{DS} = 2.6V$, $V_{GS} = 0V$ measured (\square) and modeled (solid); c) S_{21} @ $V_{DS} = -0.3V$, $V_{GS} = -0.15V$ measured (\square) and modeled (solid); S_{21} @ $V_{DS} = 0.4V$, $V_{GS} = -0.15V$ measured (\square) and modeled (solid), S_{21} @ $V_{DS} = 2.6V$, $V_{GS} = 0V$ measured (\square) and modeled (solid); d) S_{22} @ $V_{DS} = -0.3V$, $V_{GS} = -0.15V$ measured (\square) and modeled (solid); S_{22} @ $V_{DS} = 0.4V$, $V_{GS} = -0.15V$ measured (\square) and modeled (solid), S_{22} @ $V_{DS} = 2.6V$, $V_{GS} = 0V$ measured (\square) and modeled (solid).

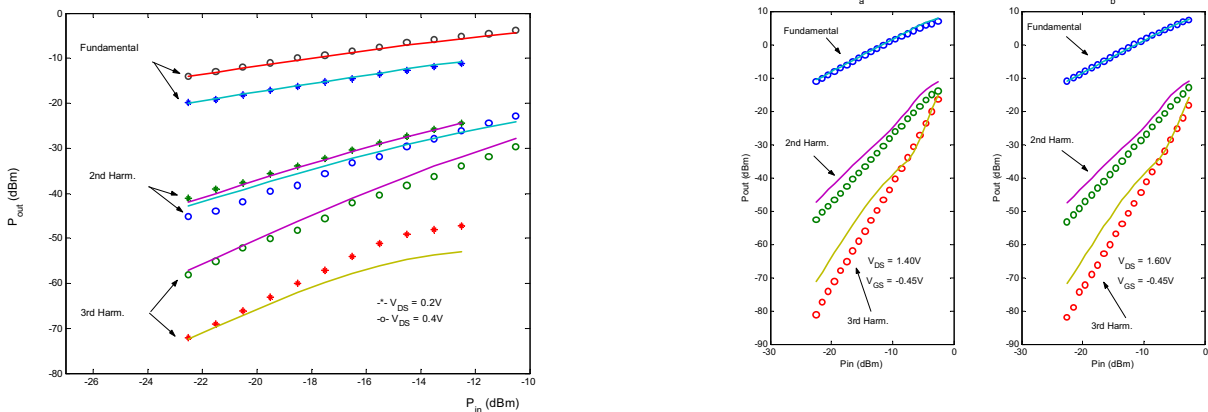


Fig. 6. Pin-Pout: Fundamental, second and third harmonic. (*) meas. at $V_{DS} = 0.2V$ and $V_{GS} = -0.45V$; (o) meas. at $V_{DS} = 0.4V$ and $V_{GS} = -0.45V$; (solid lines) model.

Fig. 7. Pin-Pout: Fundamental, second and third harmonic. (dot) measurements, (solid) model; a) $V_{DS} = 1.4V$; b) $V_{DS} = 1.6V$.